Available online at www.sciencedirect.com
SCIENCE DIRECT®
Polymer 44 (2003) 4221–4228
polymer
www.elsevier.com/locate/polymer

Incorporation of methyl acrylate in acrylonitrile based copolymers: effects on melting behavior

D. Godshall[a], P. Rangarajan[a], D.G. Baird[a], G.L. Wilkes[a,*], V.A. Bhanu[b], J.E. McGrath[b]

[a]*Department of Chemical Engineering, Virginia Polytechnic Institute and State University, Blacksburg, VA 24061-0211, USA*
[b]*Department of Chemistry, Virginia Polytechnic Institute and State University, Blacksburg, VA 24061, USA*

Received 25 November 2002; received in revised form 18 April 2003; accepted 22 April 2003

Abstract

The effects of methyl acrylate (MA) incorporation (0–15 mol%) on the glass transition, melting behavior, and the peak temperature of the stabilization exotherm in acrylonitrile (AN) based copolymers were studied. A qualitative decrease in crystalline content with increasing MA content was observed using wide angle X-ray scattering (WAXS). The lower crystallinity of the high MA content copolymers could also be noted by the magnitudes of the modulus drop at T_g using dynamic mechanical analysis (DMA) and the step change in heat capacity at T_g using differential scanning calorimetry (DSC). The DSC and differential thermal analysis (DTA) results indicated that the melting temperature of the copolymers decreased with increasing MA content. The magnitude of the crystallization exotherms decreased with successive melting/crystallization cycles. DTA experiments demonstrated that the stabilization reaction, which transforms polyacyrlonitrile into an insoluble, rigid structure, is delayed by the presence of the comonomer.

Keywords: poly(acrylonitrile); PAN; Methyl acrylate

1. Introduction

The majority of carbon fibers today are produced using either carbon pitch materials or acrylonitrile (AN) based polymers [1]. A large fraction of the cost associated with the production of AN based carbon fibers can be attributed to the solution spinning of the precursor fibers which requires the use of large amounts of toxic solvents. Therefore, the development of a melt processable AN system would substantially reduce carbon fiber prices.

Currently, a solution spinning process is used because the melting temperature of polyacyrlonitrile (PAN) [2], T_m = 317 °C, is well above the temperature at which the stabilization reaction transforms PAN into an insoluble, cross-linked material, the structure of which is typically referred to as a ladder polymer. Several mechanisms involving both intra and inter molecular pathways, as well as structures resulting from the stabilization reaction, have been suggested. It is generally agreed upon that the stabilized ladder polymer consists of short runs, approximately five, of fused rings, each containing five carbons and a single nitrogen atom along the length of the chain, with cross-links or shared rings connecting adjacent chains. A review of the literature, and proposed mechanisms for the stabilization process, has been provided by Bahsir [3]. Because the stabilized material is both cross-linked and has a very rigid backbone, the material does not flow. Therefore, the development of a *melt spinnable* PAN based carbon fiber requires a PAN material that can be processed well below the temperature at which the stabilization reaction occurs. To achieve this goal, the melting temperature of the crystalline phase in PAN must be substantially lowered from the value of 317 °C characteristic of the homopolymer.

It should be noted that currently, there exists some question as to the exact nature of the solid state structure of PAN. Several unit cells have been defined in the literature to describe the crystalline ordering observed [4–7]. In addition, commercial PAN is an unusual homopolymer in that it displays crystalline order despite being atactic. Fractions of atactic, syndiotactic, and isotactic triad runs as determined by NMR have been reported as 0.51, 0.24, and 0.25, respectively [8]. This leads to an irregular arrangement of the nitrile groups about the chain axis when the chain is

* Corresponding author. Tel.: +1-540-231-5498; fax: +1-540-231-9511.
E-mail address: gwilkes@vt.edu (G.L. Wilkes).

0032-3861/03/$ - see front matter © 2003 Published by Elsevier Science Ltd.
doi:10.1016/S0032-3861(03)00369-0

partially extended, causing many researchers to define PAN crystallites as only having lateral order in two-dimensions (perpendicular to the chain axis) rather than three. Furthermore, conflicting interpretations regarding the glass transition temperature of PAN have been reported and summarized in a separate article by Bashir [9]. The use of DSC in detecting T_g has been limited due the weakness of the transition. The lack of an obvious step change in heat capacity at T_g in PAN can be attributed to the very large breadth of the transition, as suggested by DMA, thus smearing the transition over a wide temperature range, and the fact that the homopolymer has been suggested to be approximately 50% crystalline [10]. The interpretation of DMA experiments has been complicated by the observance of two damping peaks, together which span a temperature range from roughly 50 to 170 °C, either of which have been suggested to be the T_g depending on the study [9]. The presence of the two damping peaks has been observed to depend on the orientation state of the polymer as it is not noted in well oriented fibers [9]. The investigation addressed in this report will treat PAN and its copolymers with MA as traditional semicrystalline polymers which can be adequately described by a two phase morphological model with well defined glass and melting transitions.

It is well known that the melting point of semicrystalline polymers can be reduced through the incorporation of comonomer units. This effect is analogous to the phenomenon of melting point depression observed in low molecular weight systems upon the addition of impurities or diluents. The fundamental theory which predicts the equilibrium melting point, as it applies to polymeric materials, was originally outlined by Flory [11]. No attempt in this work will be made to directly correlate experimental results with the theory, as determination of the true equilibrium melting point in materials with broad melting peaks and which are thermally unstable can be problematic. Rather, the overall goal of this study was to demonstrate that through the incorporation of a suitable type, and level of comonomer, the melting point of AN based copolymers can be reduced sufficiently to allow melt processing. This work represents a continuation of this effort [12,13].

The theoretical treatment of Flory predicts that the magnitude of melting point depression is a function of the comonomer loading, the ratio of repeat unit molar volumes, and the interaction parameter, χ, between the two types of units. However, in this application it is also important to consider the effect the comonomer has on the stabilization reaction of PAN. A substantial body of research has been published investigating this area [3,14–23]. For example, acidic comonomer groups have been demonstrated to initiate stabilization and moderate the exotherm. Comonomer units which act to lower the temperature at which stabilization occurs may be detrimental in a melt spinning scheme as they will narrow the melt processing temperature window. Here this range is defined as temperatures below which stabilization occurs, yet above the copolymer melting point. Thus for a melt spinnable PAN based copolymer, the comonomer must both retard the stabilization reaction and be incorporated at levels sufficient to reduce the melting point.

2. Experimental methods

The solution polymerization of AN and methyl acrylate (MA) was conducted by first charging a 500 ml flask fitted with a stirrer, condenser, and nitrogen purge with 50 ml of *N*-*N*-dimethyl formamide. Prior to monomer addition, the flask was purged with nitrogen for fifteen minutes. Next, the initiator, 2,2′-azo-bis-isobutyronitrile, and chain transfer agent, dodecyl mercaptan, were added to the reaction flask. Total monomer content for each polymerization was held at 375 mmol. The reactions were conducted at 70 °C for six hours. The obtained polymer was washed with a 50 fold excess of deionized water and subsequently dried for 24 h at 70 °C under vacuum. Additional details regarding the synthesis procedure can be found in a prior publication [12]. Polymers containing 0, 7, 10, and 15 mol% MA were synthesized. Individual materials will be referred to by using their AN and MA contents, respectively. Thus, the 15 mol% MA copolymer will be referred to as the 85–15 copolymer.

The final comonomer content of the materials were verified using a Varian Unity 400 ^{1}H and ^{13}C NMR. Intrinsic viscosity (IV) measurements were performed in NMP at 25 °C. Absolute molecular weight data was also obtained for the materials using a Waters 260 GPC with differential refractometer detector and an online viscometric detector coupled in parallel. The solvent used was NMP with 0.02 M P_2O_5 added to eliminate interchain association.

Thermal analysis was conducted to characterize melting behavior prior to degradation using a Seiko instruments thermo gravimetric and differential temperature analyzer (TG/DTA) with nitrogen purge and a rapid heating rate of 60 °C/min. Aluminum pans with pierced lids were used to hold the 3–5 mg samples. The use of pierced lids allowed for the escape of residual moisture. Prior to each TG/DTA experiment, the sample was conditioned by heating to 200 °C at a rate of 20 °C/min and holding for two minutes. The sample was then cooled to room temperature, again at 20 °C/min, and the experiment begun. This conditioning step, *which does not appear in any of the data plots*, was conducted to remove any residual water or solvent that may have been present and to erase any physical aging effects in the samples. A Perkin–Elmer series 7 differential scanning calorimeter (DSC) with nitrogen purge was used to study the glass transition behavior for all materials and the melting behavior of selected samples at a heating rate of 20 °C/min. As with the TG/DTA experiments, aluminum pans with pierced lids were used to hold the 3–5 mg samples. The same thermal conditioning was applied to DSC samples prior to data collection as described for the TG/DTA experiments.

Dynamic mechanical analysis (DMA) was conducted using a Seiko instruments DMS 210 at a frequency of 1 Hz with a temperature ramp of 2 °C/min under nitrogen. Film specimens for testing were prepared as follows. The copolymer in powder form was placed in a mold formed by stacking multiple layers of aluminum foil. The powder filled mold was compressed into a brittle, opaque film at room temperature under a pressure of approximately 140 MPa using a laboratory press. The mold with film was then transferred to a second press heated to a temperature of 150 °C (above T_g but below T_m). One minute was allowed for temperature equilibration before a pressure of 140 MPa was applied for an additional two minutes. The mold with film was then removed from the press and allowed to rapidly cool under exposure to room temperature. The resulting specimen thickness was approximately 0.3 mm. It is recognized that this procedure is not ideal for producing an orientation free specimen. However, it was deemed necessary to keep the temperature and time of exposure to a minimum, to prevent the onset of degradation. It should be noted that the temperature and pressure was sufficient to transform the opaque films into transparent films for the three comonomer containing materials (85/15, 90/10, and 93/7) while the homopolymer film (100/0) remained opaque. Of further note, film samples prepared using this procedure showed identical heat flow behavior in the DSC as their original powder form counterparts after the standard 200 °C conditioning step mentioned above, thereby suggesting that the film preparation process did not result in degradation of the polymer.

Wide angle X-ray scattering (WAXS) experiments were conducted on films produced in the same manner as described above for the DMA. A Philips 1720 tabletop generator was used to produce Ni filtered Cu Kα radiation of wavelength 1.54 Å. A Warhaus camera under vacuum was used to obtain flat plate photographs of the scattering patterns for exposure times of 2–4 h.

Melt viscosity measurements were made using an RMS 800 dynamic spectrometer with parallel plate geometry under nitrogen purge at 220 °C over the frequency range of 0.1 to 100 rad/s. The samples consisted of compression molded discs (25 mm diameter, 1 mm thick) produced by filling molds preheated to 200 °C and applying approximately 35 MPa in a laboratory press. These conditions of temperature and pressure were held for five minutes after which the mold was removed from the press and allowed to cool on the lab bench-top.

3. Results and discussion

3.1. Molecular weight

The values of IV and number average molecular weight (M_n) for each polymer are summarized in Table 1. The IV (NMP, 25 °C) values are between 0.49 and 0.60 dL/g, which are much lower than the range of values (1–3 dL/g) typically used in the solution spinning of PAN precursor fibers [24]. The M_n values obtained from GPC experiments range from 18,700 to 24,400 g/mol, demonstrating directly that the materials studied are of similar molecular weights. In this study, the molecular weight was intentionally kept low in an effort to produce PAN based copolymers with melt viscosities suitable for fiber spinning. Therefore, small differences in T_g and chain mobility may exist in these samples relative to the results typically noted in the literature. Of greatest importance to this study, however, the IV and GPC data indicate that as stated above each of the samples studied here are of similar molecular weight.

Table 1
Intrinsic viscosity and molecular weight data for materials studied

Material	IV (dL/g)	M_n (g/mol)
100/0	0.6	24,400
93/7	0.55	21,700
90/10	0.52	20,200
85/15	0.49	18,700

See Section 2 for measurement conditions.

3.2. DTA results

When PAN is heated to temperatures above 300 °C using modest (~10 °C/min) heating rates in a DSC or DTA experiment, the endotherm associated with melting cannot be observed because it is overwhelmed by the highly exothermic reactions associated with stabilization and degradation. This thermal event is analyzed in Fig. 1, where DTA traces for each of the materials study are presented obtained at a heating rate of 60 °C/min and normalized on sample mass. From these results it is clear that the MA units inhibit the stabilization reaction as the exotherm peak is shifted to higher temperatures with increasing comonomer content. The area associated with the exothermic event can also be observed to

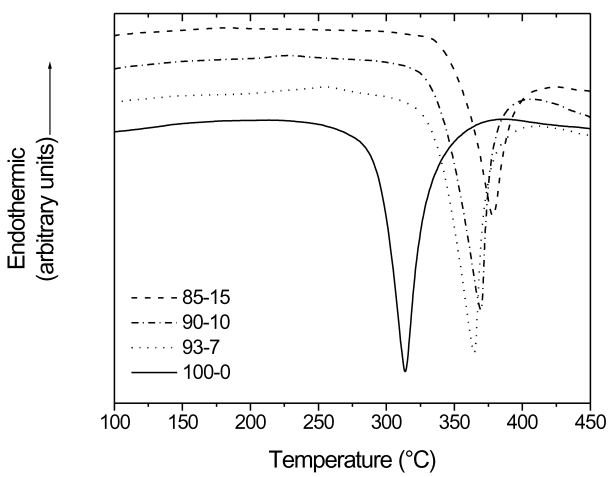

Fig. 1. DTA traces showing exothermic stabilization/degradation reactions. Heating rate 60 °C/min, nitrogen atmosphere.

decrease, suggesting that the amount of material, which undergoes transformation from these reactions, is also decreasing. While the delayed onset of these changes may prolong the time required for thermal stabilization, such a delay is required for a melt processed system as it enhances the stability of the melt at elevated temperatures.

Close inspection of the DTA traces for the MA containing materials in Fig. 1 reveals that small endothermic events can be observed prior to the main exotherm. The data below 325 °C in Fig. 1 is plotted in Fig. 2 with a rescaled *y*-axis to display these endotherms more clearly. It should be noted that the melting in pure PAN has been observed by heating sufficiently quickly such that full melting occurs prior to the rapid acceleration of the degradation kinetics [9,25,26]. However, in this study, even at the relatively rapid heating rate of 60 °C/min, the melting event is masked in the homopolymer sample. A systematic decrease in the melting temperature of the copolymer materials is observed with increasing comonomer content. With a melting temperature of 317 °C, it is readily apparent why the melting transition cannot be observed in the PAN homopolymer, as the stabilization/degradation exotherm begins to dominate the temperature differential already at 225 °C. However, this is not the case for the copolymers. As the incorporation of MA units acts to push the stabilization exotherm to higher temperatures, the MA units also depress the melting point. The combination of these two effects separates the temperature range over which melting and chemical transformation occurs sufficiently that they no longer fully overlap.

It is also interesting to note from Fig. 2 that increasing the MA content reduces the magnitude of the melting endotherm, thereby demonstrating a decrease in crystalline content. This result is expected as the incorporation of comonomer units, which cannot cocrystallize with AN, should reduce the amount of material available for crystallization by promoting a loss of chain symmetry.

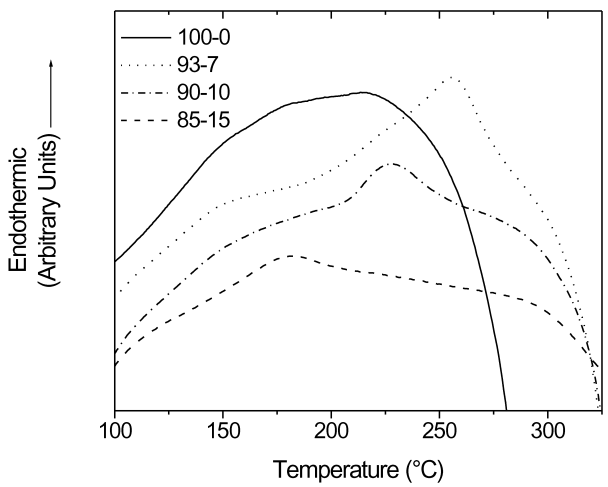

Fig. 2. DTA traces showing melting endotherms prior to the onset of exothermic stabilization/degradation reactions. Heating rate 60 °C/min, nitrogen atmosphere.

3.3. X-ray scattering

A qualitative comparison of the materials' crystalline content can be made by examining the WAXS patterns presented in Fig. 3. In the homopolymer the two sharp diffraction rings typical of PAN are evident, corresponding to scattering angles and Bragg spacings, respectively, of $2\theta = 17°$ ($d = 5.30$ Å) and $2\theta = 29°$ ($d = 3.04$ Å), superimposed over a diffuse background. Fig. 3 demonstrates that as the MA content of the polymers rises, the diffraction rings become increasingly diffuse. This suggests that the MA unit is effective in disrupting the ordered structures found in the homopolymer, thus reducing the crystalline content. Indeed, the outer diffraction ring is no longer visible in the 85–15 mol% copolymer.

3.4. Glass transition

The reduction in crystalline content resulting from the incorporation of MA units can also be observed indirectly by examining the glass transition. The results of DSC experiments normalized on sample mass used to measure T_g in these materials are plotted in Fig. 4. The step change in heat capacity associated with T_g is clearly evident in the MA containing materials. In accordance with the results of others [9], the homopolymer's T_g is not readily observed. As expected, because the T_g of polymethylacrylate [27], 10 °C, is well below that of PAN, the T_g of the respective copolymers is depressed relative to pure PAN. The incorporation of MA units systematically reduces T_g. Furthermore, the magnitude of the step change at T_g

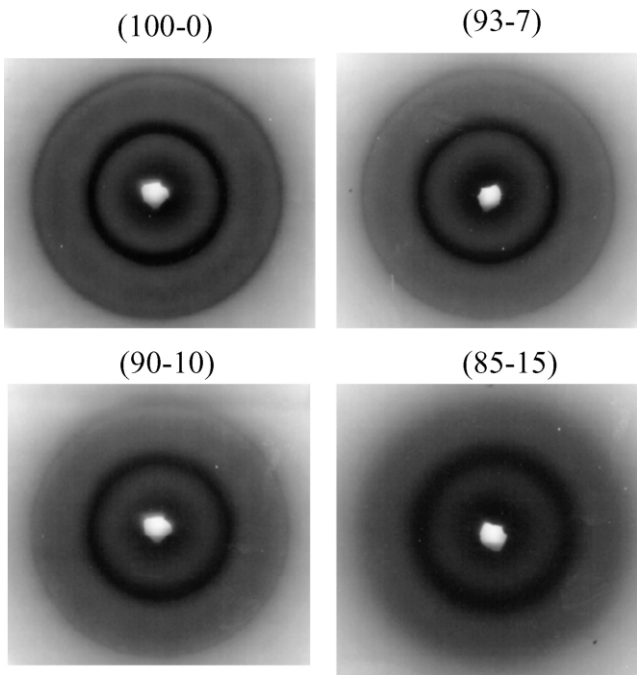

Fig. 3. WAXS negatives of materials studied. Two sharp rings ($2\theta = 17°$, $d = 5.30$ Å, and $2\theta = 29°$, $d = 3.04$ Å) are evident in the homopolymer which diminish with increasing MA content.

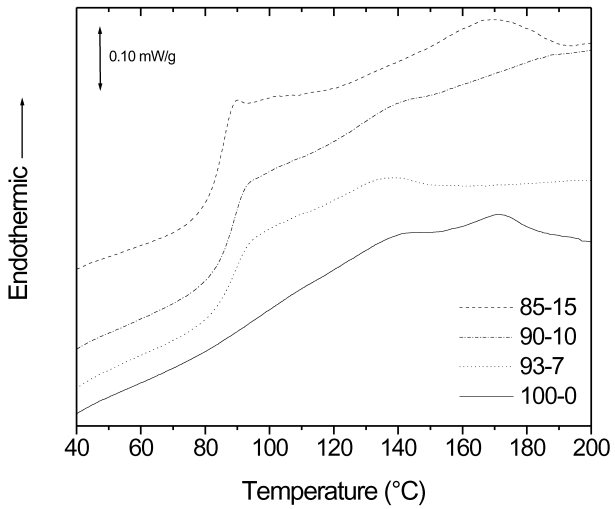

Fig. 4. DSC results demonstrating effect of MA content on the glass transition. Heating rate 20 °C/min, nitrogen atmosphere.

increases as the MA content is raised. This result further suggests that a larger amorphous fraction is found in the higher MA containing materials, or conversely, that the incorporation of MA units acts to lower crystallinity. Undulations of the heat flow signal appearing in Fig. 4 above the T_g are believed to be due to a very small fraction of highly imperfect crystallites melting and/or recrystallizing as the effect was more pronounced in samples which had been rapidly quenched from elevated temperatures to below T_g (experiments not shown).

More dramatic evidence of the reduction in crystalline content and T_g resulting from the addition of MA in these PAN based polymers can be found by examining their viscoelastic response. The results of DMA experiments for each of the materials are shown in Fig. 5. All of the samples exhibit behavior typical of polymeric materials, with a reduction in storage modulus as the temperature is raised above T_g. The magnitude of the modulus drop is observed to be a strong function of the comonomer content, with greater MA levels associated with correspondingly greater reductions in modulus. As it is the amorphous phase which undergoes dramatic softening above T_g, the DMA results clearly demonstrate that the higher MA content materials are comprised of a larger amorphous fraction than the PAN homopolymer. The damping response, associated with the magnitude of the loss tangent, further demonstrates the reduced crystalline content associated with the incorporation of comonomer units. It is also of interest to note that while not visible because of the scale used in Fig. 5, the homopolymer demonstrated two well defined, though overlapping, peaks in the loss tangent at 83 °C (smaller) and 120 °C (larger). This is in contrast to each of the copolymers, which displayed only one maximum. The two peaks are clearly evident in Fig. 6, where the loss tangent of the homopolymer has been plotted using a magnified scale as a function of temperature.

The simple Fox–Flory relationship predicts that the T_g of a statistical copolymer is a function of the relative volume fractions and homopolymer T_gs of the constituents. With a T_g of ca. 10 °C, it is expected that the MA units will depress the T_g in these copolymers relative to pure PAN. Based upon the DMA results it is not clear whether the T_g of homopolymer PAN should be assigned to either 83 or 120 °C. However, the copolymer T_gs obtained from the DMA experiments all fall *above* 83 °C (values of 102, 100, and 96 °C for copolymers 93–7, 90–10, and 85–15, respectively). Therefore, these results strongly suggest that the lower tan δ peak cannot be associated with the glass transition temperature. As such, this study finds the higher temperature peak at ca. 120 °C to be indicative of the glass transition of PAN.

The influence of MA content on the melting temperature can also be inferred from the DMA results. Sample failure in each of the copolymer materials resulted from excessive softening as the result of entering the beginning stages of the viscous flow regime. The temperature at which the rubbery

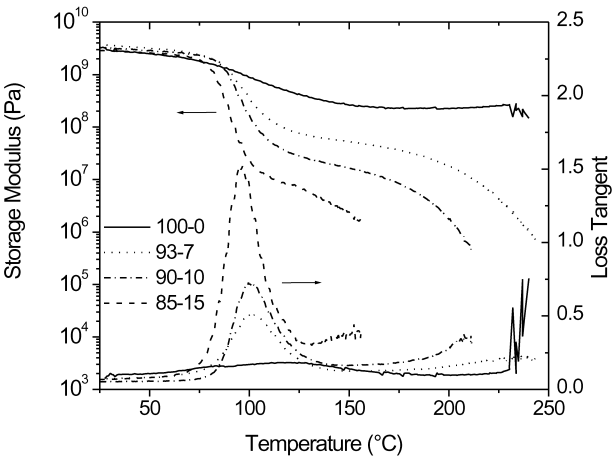

Fig. 5. Dynamic mechanical response of materials tested at 1 Hz. Heating rate 2 °C/min, nitrogen atmosphere.

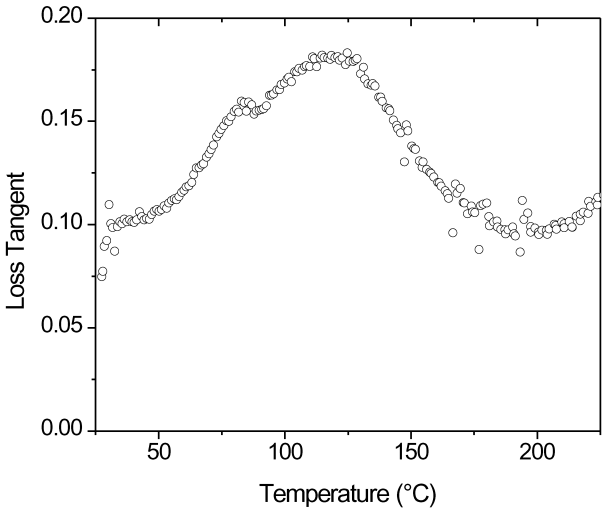

Fig. 6. Loss tangent of homopolymer tested at 1 Hz displaying dual damping peaks. Heating rate 60 °C/min, nitrogen atmosphere.

plateau ends, i.e. the melting point, varies systematically with the lowest temperature being associated with the highest MA content copolymer. The experiment was ended prior to any observation of viscous flow in the case of the PAN homopolymer.

The variation in melting temperature as a function of comonomer content can be observed quite distinctly using melt rheology. Fig. 7 compares dynamic shear viscosity measurements obtained at 220 °C. Note the huge disparity, four orders of magnitude, in viscosity between the 85–15 and 90–10 copolymers relative to the 93–7 copolymer. Recall that all of the materials studied are of similar molecular weight. This large shift in viscosity, associated with only a small change in comonomer content, can most readily be explained by returning to the DMA results. In Fig. 8 the DMA results have been replotted in terms of complex tensile viscosity, using the simple relations between dynamic viscoelastic properties [28] given in Eqs. (1)–(3) where $\bar{\eta}'$, $\bar{\eta}''$, and $\bar{\eta}^*$ and are the real, imaginary, and complex tensile viscosities, E' and E'' are the real and imaginary tensile moduli, and ω is the testing frequency. Thus, the data in Fig. 8 demonstrate how the complex viscosity varies as a function of temperature. Comparing the data at 220 °C, the temperature corresponding to the melt viscosity results in Fig. 7, it becomes readily evident that the four orders of magnitude reduction in viscosity observed between the 93–7 and 90–10 copolymers arises because at 220 °C, the 93–7 copolymer has not fully entered the viscous flow regime in contrast to the 90–10 copolymer. Thus the importance of achieving full melting in these copolymers to facilitate melt processing in these materials should be noted.

$$\bar{\eta}' = \frac{E''}{\omega} \tag{1}$$

$$\bar{\eta}'' = \frac{E'}{\omega} \tag{2}$$

$$|\bar{\eta}^*| = \lfloor(\bar{\eta}')^2 + (\bar{\eta}'')^2\rfloor^{1/2} \tag{3}$$

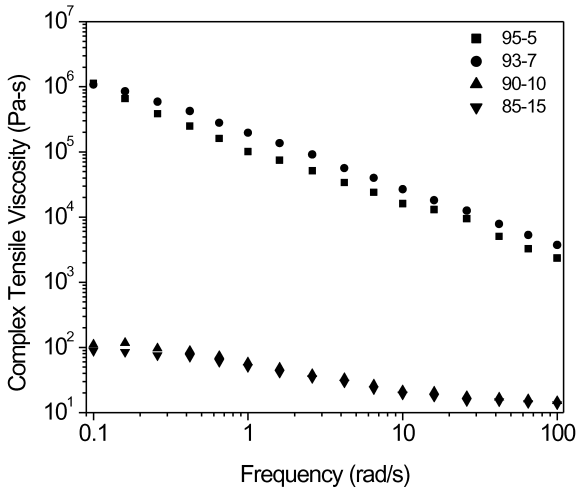

Fig. 7. Complex shear viscosity of material determined using parallel plate dynamic rheology at 220 °C. Note four orders of magnitude decrease in viscosity between 93–7 and 90–10 copolymers at low shear rates.

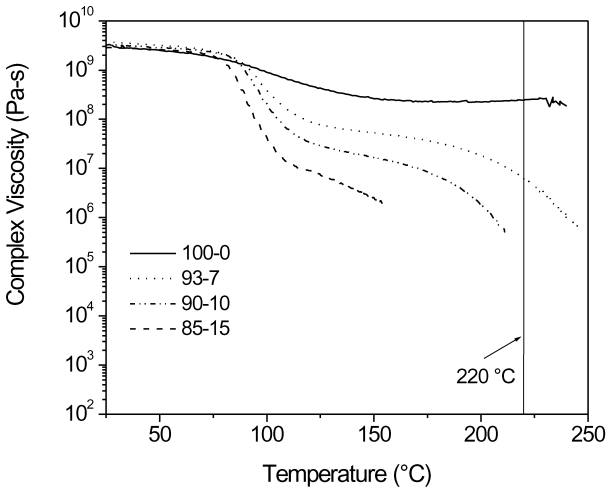

Fig. 8. Complex tensile viscosity of material determined using DMA data at 1 Hz. Vertical line demarks 220 °C, the temperature at which the complex viscosity data of Fig. 7 was obtained.

The DMA results yield complex viscosity values that are somewhat larger than those obtained in the rheology experiments. In accordance with the different geometries employed in the two experiments, tension and shear for the DMA and rheometry experiments, respectively, it is to be expected that the DMA results will be greater by a factor of three. However, this adjustment does not fully account for the larger values obtained in the DMA. It is believed that the slow heating rate employed in the DMA experiments, 2 °C/min, may have resulted in a partial branching or cross-linking, due to stabilization, during data collection. As the rheometry experiment, encompassing only one temperature, was shorter in duration, the effects of chemical transformation were undoubtedly less severe.

3.5. Melting and crystallization

To further establish that the observations made in the proceeding experiments could be attributed to melting, additional experiments were conducted using DSC to demonstrate the reversible nature of the transition. In addition, because the stabilization reaction, and subsequent formation of ladder structures, reduces the fraction available for crystallization, the reproducibility of the melting-crystallization behavior with successive heating-cooling cycles should provide an indirect indication of the thermal stability of these materials.

Three melting and crystallization cycles are shown in Fig. 9 for the 85–15 copolymer. A heating rate of 20 °C/min was employed, and upon reaching 200 °C in the middle of each cycle the sample was held for 2 min to facilitate the full melting of residual nuclei. Comparing the results from successive cycles it is evident that the melting, crystallization, and glass transitions are unchanged from one cycle to the next. It should be emphasized that in this experiment, as well as with the other DSC results presented, no low

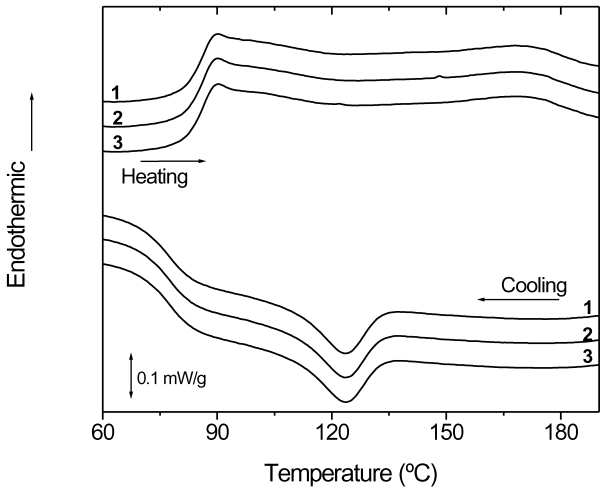

Fig. 9. DSC traces for copolymer 85–15 through three successive melting and crystallization cycles. Heating rate 20 °C/min, 2 min hold at 200 °C in the middle of each cycle.

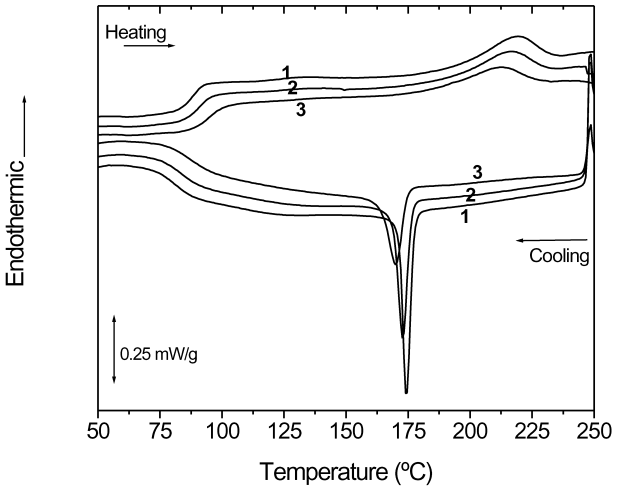

Fig. 11. DSC traces for copolymer 90–10 through three successive melting and crystallization cycles. Heating rate 20 °C/min, 2 min hold at 250 °C in the middle of each cycle.

molecular weight diluents or plasticizers were used. This is in contrast to studies which observe melting via DSC using water plasticized materials in sealed pans [16,29,30].

A more rigorous test of the thermal stability was made by increasing the maximum temperature encountered in each cycle. An identical experiment with the 85–15 copolymer was conducted in which the material was held for 2 min at 250 °C at the end of each heating cycle. The results of this experiment are plotted in Fig. 10. A subtle decrease in the magnitude of the crystallization exotherm in addition to an increase in T_g from 85 °C in the first cycle to 88.5 °C in the third occurs. These changes are consistent with the formation of rigid material, the ladder structure, as a result of cyclization, at the expense of crystallizable material.

In Fig. 11, the DSC results for three thermal cycles of the 90–10 copolymer are plotted. Beginning with the first heating/cooling cycle, it is evident that the 90–10 mol% contains a much higher crystalline content than the 85–15 mol% because of its comparatively larger melting and crystallization peaks. Unlike the 85–15 material, the 90–10 copolymer shows a dramatic reduction in crystalline content with each successive heating/cooling cycle, most clearly demonstrated by the shrinking of the crystallization exotherm. The previous DTA results plotted in Fig. 1 demonstrated the inhibitory effect that MA incorporation has on the stabilization exotherm. Thus, with a lower MA content, the 90–10 copolymer undergoes a more rapid chemical transformation than the 85–15 copolymer at 250 °C.

The importance of stabilization kinetics in determining the melt stability of these materials is further emphasized by the data provided in Fig. 12. In this experiment, the 90–10 copolymer underwent the same thermal cycling as applied in Fig. 11 with one modification. Rather than holding for

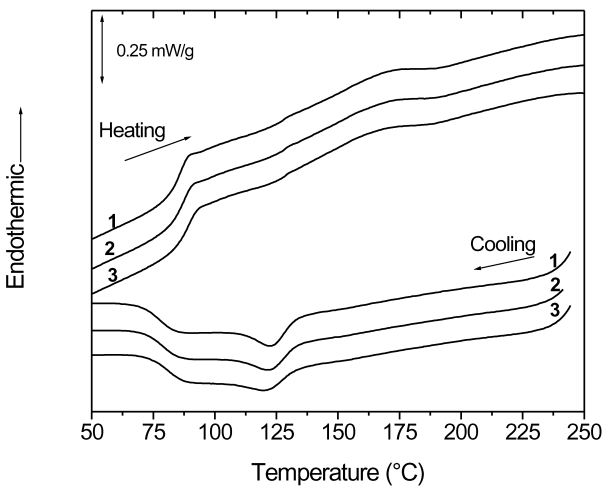

Fig. 10. DSC traces for copolymer 85–15 through three successive melting and crystallization cycles. Heating rate 20 °C/min, 2 min hold at 250 °C in the middle of each cycle.

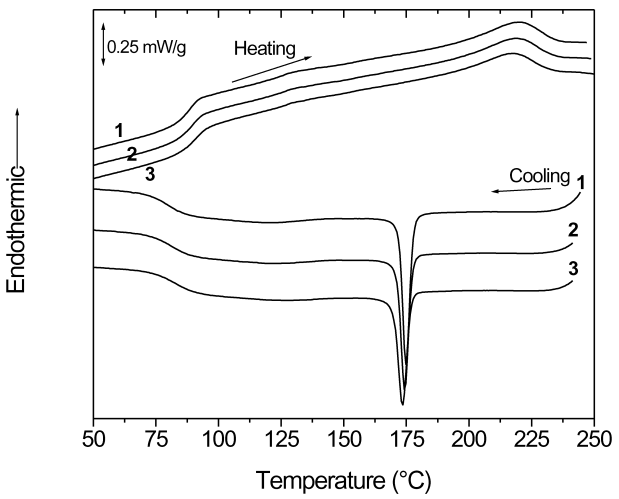

Fig. 12. DSC traces for copolymer 90–10 through three successive melting and crystallization cycles. Heating rate 20 °C/min, 0.5 min hold at 250 °C in the middle of each cycle.

2 min at 250 °C in the middle of each thermal cycle, the DSC experiment plotted in Fig. 12 involved 30 s holds at 250 °C. Thus, the time spent at elevated temperatures has been reduced in Fig. 12 relative to Fig. 11. With the shorter dwell time at 250 °C the 90–10 copolymer demonstrates greater reproducibility of the melting and crystallization transitions from one thermal cycle to the next.

Similar DSC experiments for the lower MA content materials were not possible as the higher temperatures required to achieve melting, and the faster reaction kinetics, precluded the observation of melting/crystallization behavior over multiple cycles. That is, after the initial melting, only a very small fraction of the material remained pristine and suitable for crystallization.

4. Conclusions

The thermal and structural characteristics of a series of PAN-co-MA polymers were studied. Several techniques; WAXS, DTA, DSC, and DMA demonstrated that the crystalline content and the T_g of the materials were reduced as greater levels of MA were incorporated. In addition, greater levels MA acted to lower the melting temperature of the copolymers. Accompanying this decrease in melting point was an inhibition in the kinetics of the stabilization/-degradation reactions, which occur in PAN at elevated temperatures. Chemical changes in the materials as a result of these reactions were inferred from the effects of residence time and temperature on the reproducibility of the melting and crystallization transitions with thermal cycling. Thus, the time–temperature window of melt stability was demonstrated to increase with the incorporation of greater levels of the MA comonomer. This window must be made broad to achieve a melt spinnable PAN based system which is sufficiently robust to withstand extended times at elevated temperatures within an extruder.

References

[1] Riggs JP. Encyclopedia of polymer engineering and science. Carbon fibers. Ed. J.I. Kroschwitz. Wiley-interscience New York. vol. 2. p. 641, 1985.
[2] Krigbaum WR, Tokita N. J Polym Sci 1960;43:467.
[3] Bashir Z. Carbon 1991;29(8):1081.
[4] Lindenmeyer PH, Hosemann R. J Appl Phys 1963;34(1):42.
[5] Bashir Z. J Polym Sci, Part B: Polym Phys 1994;32:1115.
[6] Bashir Z, Church SP, Waldron D. Polymer 1994;35(5):967.
[7] Yamane A, Sawai D, Kameda T, Kanamoto T, Ito M, Porter R. Macromolecules 1997;30:4170.
[8] Sawai D, Yamane A, Kameda T, Kanamoto T, Ito M, Yamazaki H, Hisatani K. Macromolecules 1999;32:5622.
[9] Bashir Z. J Macromol Sci—Polym Phys 2001;B4(1):41.
[10] Brandrup J, Immergut EH, Grulke EA, editors. Polymer handbook, 4th ed. New York: Wiley; 1999.
[11] Flory PJ, Principles of polymer chemistry, Ithaca: Cornell University Press; 1953.
[12] Rangarajan P, Bhanu VA, Godshall D, Wilkes GL, McGrath JE, Baird DG. Polymer 2002;43:2699.
[13] Rangarajan P, Yang J, Bhanu V, Godshall D, McGrath J, Wilkes G, Baird D. J Appl Polym Sci 2002;85:69.
[14] Bhat GS, Peebles IH, Abhiraman AS, Cook FL. J Appl Polym Sci 1993;49:2207.
[15] Thompson EV. Polym Lett 1966;4:361.
[16] Bajaj P, Sreekumar K, Sen K. Polymer 2001;42:1707.
[17] Bhat GS, Cook FL, Abhiraman AS, Peebles LH. Carbon 1990; 28(2/3):377.
[18] Ko T-H, Ting H-Y, Lin C-H. J Appl Polym Sci 1988;35:631.
[19] Houtz RC. Text Res 1950;20:786.
[20] Burlant WJ, Parsons JL. J Polym Sci 1956;22:249.
[21] LaCombe EM. J Polym Sci 1957;24:152.
[22] Olive GH, Olive S. Polym Bull 1981;5:457.
[23] Grassie N, McGuchan R. Eur Polym J 1971;7:1357.
[24] Gupta AK, Paliwal DK, Bajaj P. J Macromol Sci—Rev Macromol Chem Phys, Part C 1991;C31(1):1.
[25] Frushour BG. Polym Bull 1984;11:375.
[26] Dunn P, Ennis BC. J Appl Polym Sci 1970;14:1795.
[27] Brandup J, Immergut EH, editors. Polymer handbook, 2nd ed. New York: Wiley; 1975.
[28] Aklonis JJ, MacKnight WJ, 2nd ed. Introduction to polymer viscoelasticity, New York: Wiley; 1983.
[29] Frushour BG. Polym Bull 1981;4:305.
[30] Frushour BG. Polym Bull 1982;7:1.